

Evaluation of GIS-based multicriteria decision analysis and probabilistic modeling for exploring groundwater prospects

Sasmita Sahoo · Madan K. Jha · Niraj Kumar ·
V. M. Chowdary

Received: 4 November 2013 / Accepted: 20 February 2015 / Published online: 22 March 2015
© Springer-Verlag Berlin Heidelberg 2015

Abstract Quantification of groundwater resources is indispensable for developing an efficient strategy for sustainable groundwater management. Integration of remote sensing (RS) and geographical information system (GIS) techniques with multicriteria decision analysis (MCDA) has emerged as a powerful tool for the economical and rapid assessment of groundwater resources at a macroscale. The main intent of this study is to evaluate the performance of two GIS-based approaches, namely MCDA as Approach I and probabilistic modeling as Approach II for groundwater prospecting. In Approach I, the thematic layers and their features relevant to groundwater prospect were extracted using RS and GIS, and appropriate weightages were assigned to individual layers and their features based on the analytic hierarchy process (AHP) scale. After the normalization of these weights, the selected thematic layers were integrated in the GIS environment to generate a groundwater prospect map. In Approach II, two probabilistic models, viz. frequency ratio (FR) and weight of evidence (WOE), were used. The FR and WOE probability values were calculated for each of the selected themes and then groundwater prospect maps were generated by overlaying the themes in GIS. The groundwater prospect maps thus obtained by the two approaches were classified into four distinct groundwater potential zones.

These maps were verified using the available well-yield data. The verification results indicated that out of the AHP, FR and WOE techniques, the AHP technique is superior (prediction accuracy of 77 %) to the probabilistic models (FR and WOE), though the WOE model also performed reasonably well with a prediction accuracy of 73 %. It is concluded that for more reliable results, the AHP technique can be used for assessing groundwater potential in a given area/region. The findings of this study are useful for the cost-effective identification of suitable well locations as well as for the efficient planning and development of groundwater resources.

Keywords Groundwater prospecting · Geospatial techniques · Multicriteria decision analysis · Probabilistic modeling · Analytic hierarchy process · Frequency ratio · Weight of evidence

Introduction

In view of increasing demand for freshwater for various purposes such as agricultural, domestic and industrial, a greater emphasis is being laid for a planned and optimal utilization of groundwater resources. Unfortunately, the mismanagement of this valuable resource has created not only serious groundwater depletion and pollution problems, but also water supply problems for both present and future generations (Mays 2013). In addition, groundwater depletion (reduction in groundwater storage) problems has resulted in other allied problems like extensive land subsidence, reduction in stream/river flows and spring discharges, loss of wetlands and deterioration of groundwater quality. It is, therefore, imperative to make a quantitative estimation of available groundwater resources at a basin or sub-basin scale. In this regard, groundwater prospect mapping can play

S. Sahoo (✉) · M. K. Jha · N. Kumar
AgFE Department, Indian Institute of Technology Kharagpur,
Kharagpur 721 302, West Bengal, India
e-mail: sasmitait@gmail.com

M. K. Jha
e-mail: madan@agfe.iitkgp.ernet.in

V. M. Chowdary
Regional Remote Sensing Centre, East-Kolkata, NRSC,
Kolkata 700 156, West Bengal, India
e-mail: muthayya.chowdary@gmail.com

an important role in the identification of zones with probable occurrence of groundwater as it provides a rational picture of hidden freshwater resources. Nowadays, the delineation of groundwater potential zones is becoming increasingly important for successfully implementing groundwater protection and management programs.

Conventional approach of groundwater exploration using geological, hydrogeological and geophysical methods normally involve high budget, and hence are uneconomical and time consuming for large-scale investigations (Sander et al. 1996). In addition, these methods of investigation do not always account for the various factors that control the occurrence and movement of groundwater (Oh et al. 2011). Remote sensing (RS) and the geographical information system (GIS) with their advantages of spatial, spectral and temporal availability and manipulation of data covering large and inaccessible areas within a short time have become very handy tools in accessing, monitoring and conserving groundwater resources (Jha and Peiffer 2006; Jha et al. 2007; Meijerink 2007; Rodell et al. 2009; Moiwo et al. 2011; Scanlon et al. 2012; Voss et al. 2013). Moreover, remote sensing is one of the main sources of information about the surface (hydrological) features related to groundwater such as lineament, soil, topography, land use/land cover and landforms. Such spatial data and information can be easily input to a GIS environment for integration with other types of data/information followed by suitable data analyses and mapping (Hinton 1996; Jha et al. 2007).

The application of remote sensing and GIS with or without multicriteria decision analysis for the exploration/mapping of groundwater prospect zones has been reported by a number of researchers across the world (e.g., Krishnamurthy et al. 1996; Sander et al. 1996; Saraf and Choudhury 1998; Jaiswal et al. 2003; Sener et al. 2005; Solomon and Quiel 2006; Srivastava and Bhattacharya 2006; Tweed et al. 2007; Madrucci et al. 2008; Chowdhury et al. 2009; Jha et al. 2010; Machiwal et al. 2011; Jasrotia et al. 2013).

However, studies on groundwater prospect mapping using GIS and probabilistic approaches are very limited. Although the frequency ratio (FR) and weight of evidence (WOE) probabilistic models have been applied and compared to examine landslide susceptibility mapping (e.g., Lee and Choi 2004; Lee and Dan 2005; Oh et al. 2009, 2010; Pradhan and Lee 2010), ground subsidence hazard mapping (Kim et al. 2006; Lee et al. 2010), very few studies have been reported till date as far as the mapping of groundwater prospect using probabilistic approaches is concerned. Oh et al. (2011) used GIS and FR model to map regional groundwater potential in the area of Pohang City, Korea. The thematic layers used included specific capacity, transmissivity, topography, lineament, geology, forest and soil data for mapping groundwater productivity potential. Lee et al. (2012) produced the regional groundwater productivity potential map for the bedrock aquifer of Pohang City, Korea, using GIS and WOE model and

the same thematic layers as used by Oh et al. (2011). On the other hand, Ozdemir (2011) performed a comparative evaluation of FR, WOE and logistic regression models for mapping spring potential in the area of Sultan Mountains of Konya, Turkey. Seventeen spring-related parameter layers of the study area, viz., geology, fault density, distance to fault, lithologies, elevation, slope aspect, slope steepness, curvature, plan curvature, profile curvature, topographic wetness index, stream power index, sediment transport capacity index, drainage density, distance to drainage, land use/cover and precipitation were used to generate spring potential map of the study area. The results indicated that the FR and WOE models were relatively good estimators of spring potential mapping in the study area as compared to logistic regression.

It is obvious from the review and literature that most of the studies on application of RS and GIS technologies in the delineation of groundwater prospect have evaluated single method/approach only: either multicriteria decision analysis (MCDA) method (simple or AHP-based) or probabilistic method. To the best of the authors' knowledge, there has been no comprehensive study to date concerning application of probabilistic modeling and comparative evaluation of MCDA and involving the application, assessment and comparison of both MCDA and probabilistic modeling approaches for mapping groundwater prospect. Therefore, there is a need for such studies so as to identify suitable method(s) for groundwater prospecting that can provide a high predictive accuracy. The present study demonstrates the efficacy and usefulness of two GIS-based approaches, viz., MCDA approach and probabilistic modeling approach, for the identification and delineation of groundwater prospect zones. To achieve this goal, the Kushabhadra–Bhargavi groundwater basin of Mahanadi Delta, Odisha, eastern India, was considered as the study area. The first approach includes integration of a multicriteria decision analysis technique, namely analytic hierarchy process (AHP) with remote sensing and GIS to identify groundwater prospect zones in the study area. The second approach includes GIS and two probabilistic models (FR and WOE) for the identification of groundwater prospect zones in the study area.

Methodology

Study area

Location and hydrometeorology

The study area selected for the present study is Kushabhadra–Bhargavi groundwater basin, which is situated in the Mahanadi Delta Stage-II region, Odisha, eastern India (Fig. 1). It is spread mostly in the Puri and Khurdha (to some extent) districts of Odisha. The salient information about the study area is summarized in Table 1.

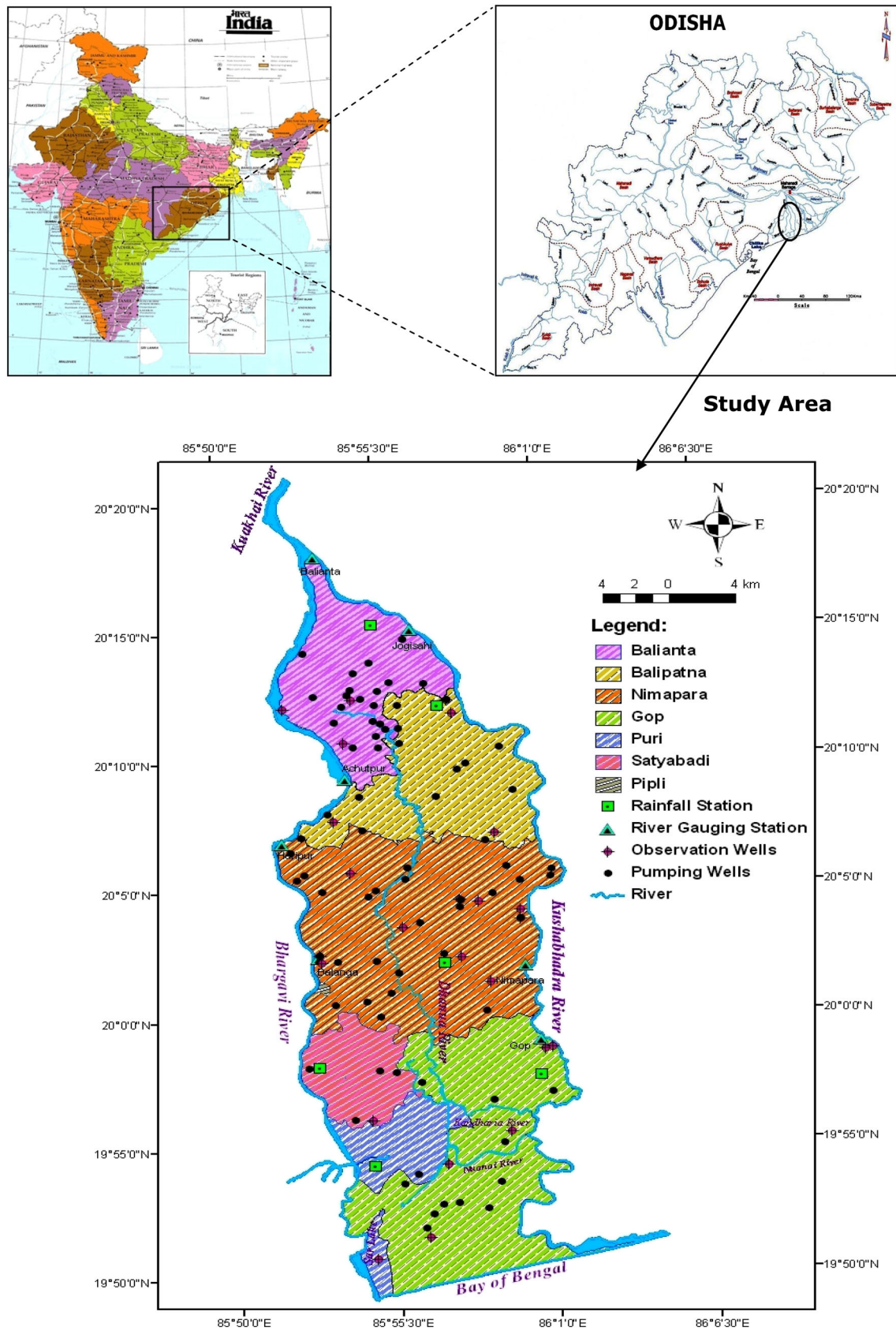


Fig. 1 Location map of the study area

Table 1 Description of the study area

Latitude	19°49′04″N–20°18′45″N
Longitude	85°54′47″E–86°03′26″E
Geographical area	620 km ²
Cultivable command area	280 km ²
Topography	Almost flat
Climate	Tropical monsoon climate
Average annual rainfall	1470 mm
Monthly maximum temperature	29–46 °C
Monthly minimum temperature	12–24 °C
Monthly humidity	41–86 %
Monthly wind speed	2.6–26 km/h

The average annual rainfall in the study area is about 1470 mm and mostly occurs during monsoon season from mid-June to the end of October. The rainfall during the months of June, July, August, September and October is about 15, 27, 26, 17 and 6 % of the annual rainfall, respectively. Three distinct seasons prevail in the area. The winter season starts from November and lasts up to the end of February; the summer season extends from March to the middle of June; and the monsoon (rainy) season from mid-June to the end of October. During the monsoon period, the area experiences heavy rainfall from the southwest monsoon. The spring, autumn and dew seasons are of very short duration and are telescoped into the three major seasons.

Sources of water supply

Among the various sources of surface water, canal is the most important source of irrigation in the study area. Canal irrigation accounts for about 280 km² of the area, with the remaining supply from other sources such as river-lift, ponds or tube wells. However, the amount of area under canal irrigation has a decreasing trend with an increase in the size of land holding because of the fact that the more affluent farmers have access to relatively expensive, but dependable sources of water supply. Exploitation of groundwater is desirable to: (1) supply additional water during dry periods, (2) relieve stress on reservoirs for irrigation during low rainfall years and (3) protect wet period crops from long dry spells during the rainy season. The aquifer system of the Mahanadi delta offers an important additional source of water resource, which needs to be utilized efficiently so as to ensure sustainable water supply in the study area.

Collection of data and extraction of relevant themes

To investigate groundwater characteristics in the study area, the pre-monsoon and post-monsoon groundwater depth data of 24 observation wells (Fig. 1) for the 1997–2011 period were collected from the Central

Groundwater Board (CGWB), Bhubaneswar, and Groundwater Survey and Investigation (GWS&I), Bhubaneswar, Government of Odisha. Groundwater potential is governed by a variety of surface and subsurface factors such as topography, land use/land cover, geology, soil, drainage density, slope, stream network, rainfall, climate, recharge, lineament and human activities, among others.

On the basis of availability of spatial and field-measured data in the study area, the themes (factors) influencing groundwater occurrences were selected for identifying groundwater prospect zones. The selected themes of the study area, viz., geology, soil, elevation, slope, drainage density and land use/land cover, were generated using both remote sensing and conventional data. The geology map, soil map and land use/land cover map of the study area at a scale of 1:250,000 were collected from Odisha Space Applications Centre (ORSAC), Department of Science and Technology, Government of Odisha. The DEM of the study area extracted from Shuttle Radar Topography Mission (SRTM) was used for generating topographic elevation, slope and drainage density maps of the study area. Moreover, the drainage network map was generated from the Survey of India toposheets (scale 1:50,000). Apart from the above spatial data, the discharge data of 77 pumping wells over the study area were collected from Orissa Lift Irrigation Corporation (OLIC), GWS&I, Bhubaneswar, Government of Odisha. The location of the pumping wells is shown in Fig. 1.

Identification and delineation of groundwater prospect zones

Thematic layers of geology, land use/land cover, soil, slope and drainage density were used for the identification and delineation of groundwater prospect zones in the study area. In this study, two approaches were used for identifying groundwater prospect zones. In Approach I, multicriteria analysis technique AHP and GIS technique were employed, whereas in Approach II two probabilistic models, namely FR and WOE along with the GIS technique, were used. The procedures of these two approaches are described in the subsequent sections.

Approach I: groundwater prospect zoning using AHP and GIS

The methodology adopted for the preparation of a groundwater prospect map using Approach I is presented in Fig. 2. After generating the above-mentioned five thematic layers of the study area, the importance of their features from groundwater viewpoint was taken into consideration and accordingly suitable weights were assigned to each thematic layer and the features of individual thematic layers. For the assignment of weights, the comparison

Fig. 2 Protocol of the methodology adopted for the preparation of groundwater prospect map using Approach I

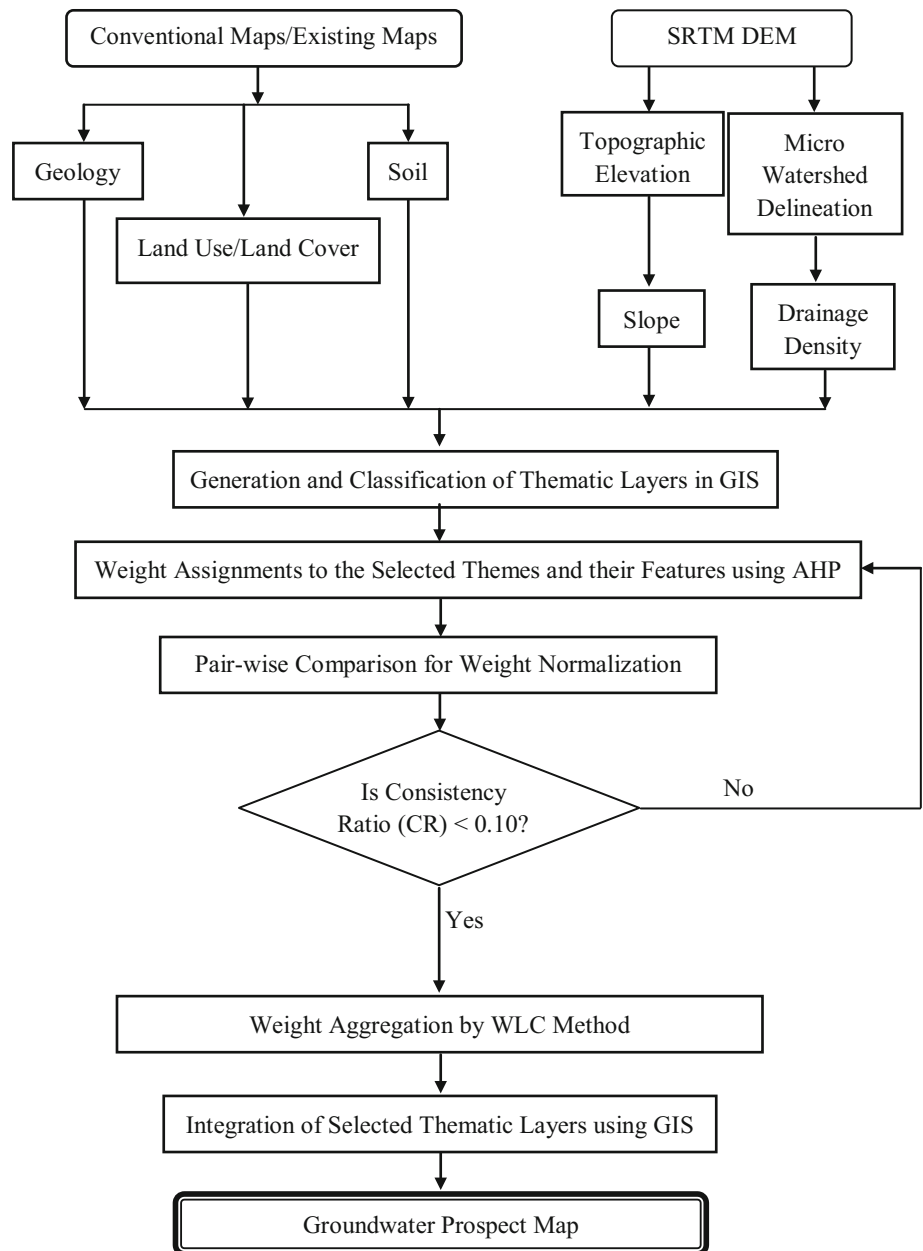


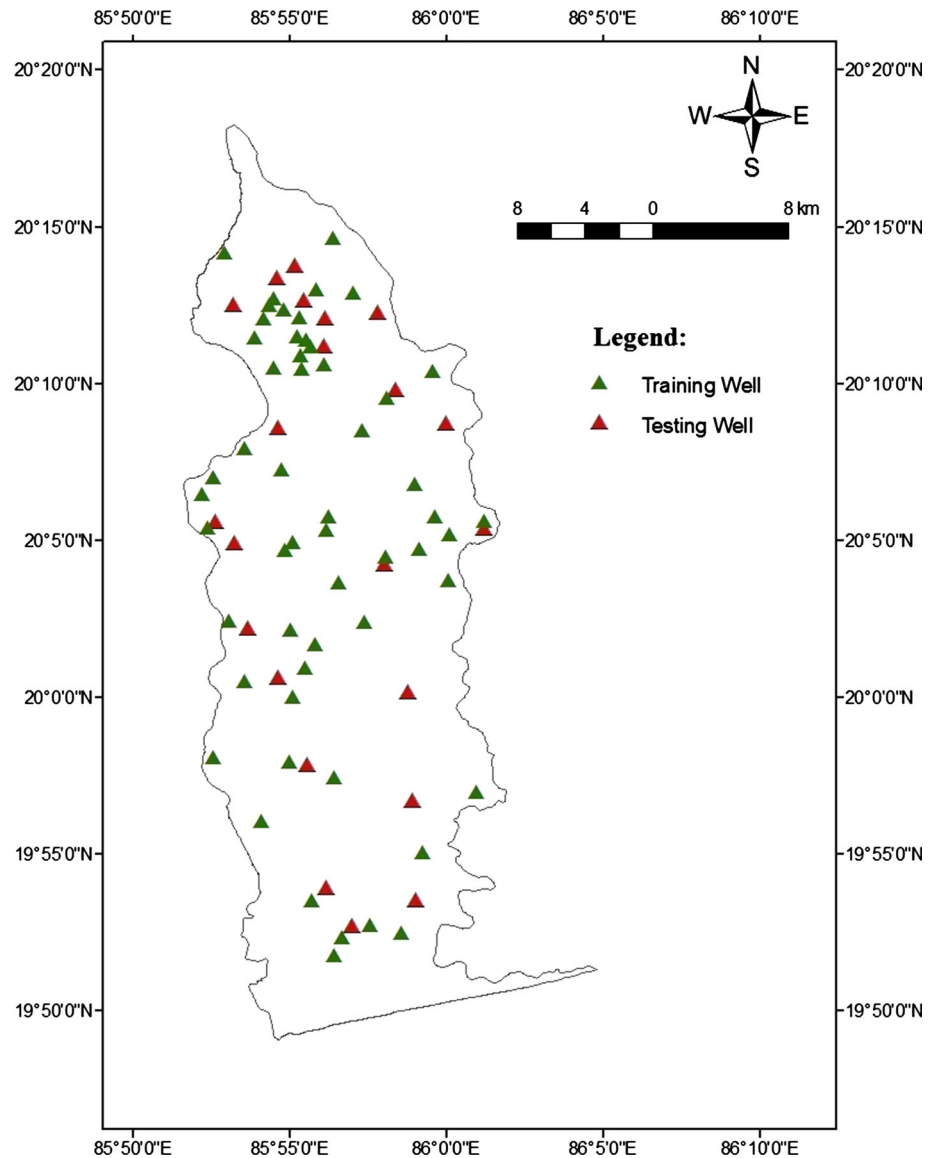
Table 2 AHP scale and its interpretation (Saaty 2001; Eastman 2003)

Less important				Equally important	More important			
Extremely	Very strongly	Strongly	Moderately	1	Moderately	Strongly	Very strongly	Extremely
1/9	1/7	1/5	1/3	1	3	5	7	9

judgment scale of Saaty (1980) as shown in Table 2 was used and the opinions of the experts were sought. One pairwise comparison matrix was developed for the comparison of the thematic layers and five pairwise comparison matrices were developed for the comparison of the features of individual thematic layers. Thereafter, normalized

weights were calculated by the geometric mean method and the consistency ratio (CR) was calculated for all the thematic layers and their individual features to check the consistency of the weights assigned. Further, all the five raster thematic layers (geology, land use/land cover, soil, slope, drainage density) were introduced in ArcView GIS

Fig. 3 Location of training and testing wells of the study area



as a grid layer. All the thematic layers were resampled to a grid size of IRS-1D-LISS-III image resolution 23.5×23.5 m. Arithmetic model for spatial raster data was developed for the integration of thematic layers using ArcView 3.2 software. The total weights of each grid (polygon) of the final integrated raster layer were derived by the weighted linear combination method expressed as follows:

$$GWPI = GG_w GG_{wi} + LU_w LU_{wi} + ST_w ST_{wi} + SL_w SL_{wi} + DD_w DD_{wi} \quad (1)$$

where GWPI is the groundwater potential index for a polygon, GG the geology, LU the land use/land cover, ST the soil type, SL the slope, DD the drainage density, 'w' the normalized weight of a theme and 'wi' the normalized weight of the individual features of a theme.

Approach II: groundwater prospect zoning using probabilistic models and GIS

In this approach, groundwater prospect maps were prepared by the FR and WOE probabilistic models. These models require the data on location of pumping wells over the study area, together with the thematic layers having significant influence on groundwater occurrence. A well location map (Fig. 3) was prepared depicting 77 pumping wells over the study area, out of which 55 were used as training wells and the remaining 22 were used as testing wells. The training wells were used in the FR and WOE probabilistic models, and the results were then implemented over the entire study area, including the test area. The testing wells were used solely for the verification of the modeling results. The selected thematic layers were

overlaid with the well location map. On the basis of these intersections, the FRs and WOE probability (P) values were calculated for each of the thematic layers. The step-by-step procedures for the application of these two probabilistic models are presented below.

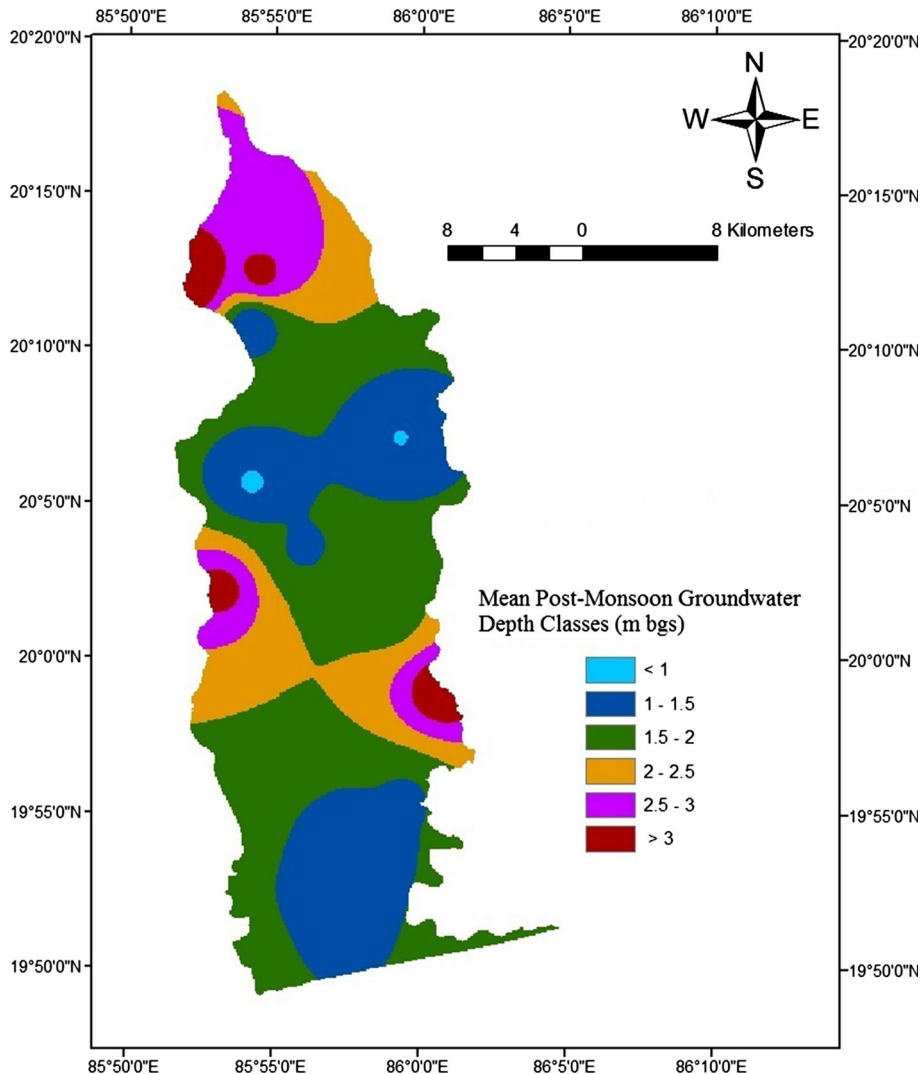
1. Frequency ratio modeling

Frequency ratio is the probability of occurrence of a certain attribute (Bonham-Carter 1994). For groundwater prospecting, FR indicates the quantitative relationship between well occurrence and different causative parameters (i.e., factors). For determining the FR of groundwater potential, the ‘area ratio’ and ‘well occurrence ratio’ were calculated for different classes of each factor (thematic layer). Thereafter, FR for different classes of each factor was calculated by dividing the ‘well occurrence ratio’ with the ‘area ratio’. These FR values were used for generating a groundwater prospect map of the study area using the

overlay function of GIS. The step-by-step procedures for FR modeling to delineate groundwater prospect zones are as follows:

- Step 1: selection of thematic layers and the preparation of thematic maps.
- Step 2: preparation of well location map and the selection of training and testing wells.
- Step 3: overlaying of the thematic maps with the training well map.
- Step 4: identification of pixels under different classes of a given factor (thematic layer).
- Step 5: computation of ‘area ratio’ for a particular class of a given factor by dividing the total number of pixels present in that class with the total number of pixels present in the study area.
- Step 6: calculation of ‘well occurrence ratio’ for a particular class of a given factor by dividing the number

Fig. 4 Mean post-monsoon groundwater depth map of the study area



of training wells present in that class with the total number of training wells present in the study area.

Step 7: calculation of FRs for each class of a given factor by dividing the ‘well occurrence ratio’ with the ‘area ratio’.

Step 8: overlaying of the thematic layers and the computation of groundwater potential index (GWPI) over the study area. The pixel-wise GWPI over the study area was computed as follows:

$$GWPI = \sum_{i=1}^N (FR)_i \quad (2)$$

where FR is the frequency ratio of the i th factor and N is the total number of factors.

Step 9: preparation of a groundwater prospect map of the study area in the GIS environment based on the range of GWPI values over the study area.

Step 10: validation of the prepared groundwater prospect map using testing wells.

2. Weight of evidence modeling

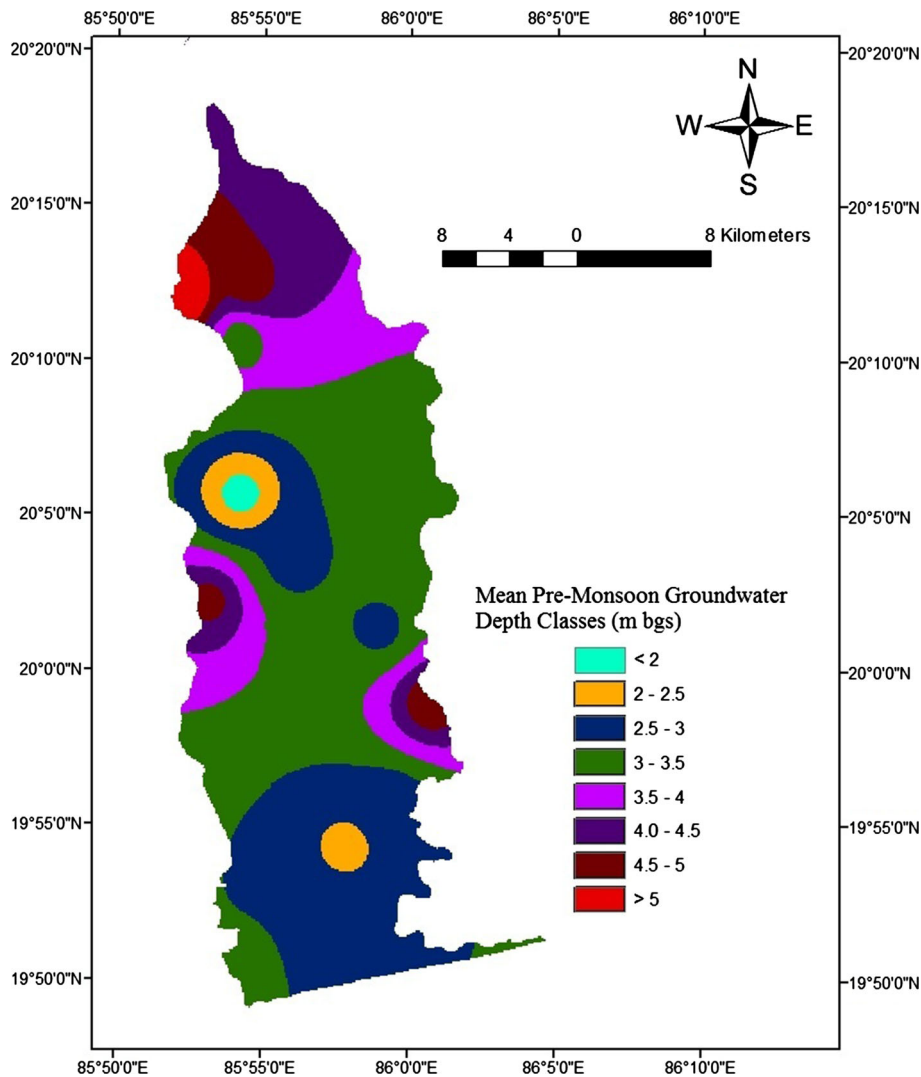
The weight of evidence model calculates the weights for groundwater prospecting based on the presence or absence of wells in each groundwater influencing factors. Like the FR model, this model also requires a set of training and testing wells. The selected groundwater-related thematic layers were overlapped with the map depicting training wells. On the basis of these intersections, weight and WOE probability values were calculated for the individual classes of different thematic layers. The step-by-step procedures for WOE modeling to delineate groundwater prospect zones are as follows:

Step 1: selection of thematic layers (factors) and the preparation of thematic maps.

Step 2: preparation of well location map and the selection of training and testing wells.

Step 3: overlaying of the thematic maps with the training well map.

Fig. 5 Mean pre-monsoon groundwater depth map of the study area



Step 4: identification of the pixels under different classes of a given factor (theme).

Step 5: calculation of weights (W^+) for each class of a theme. Weights for the individual classes of different themes were calculated as:

$$W^+ = \ln \left[\frac{\frac{\text{Number of Wells in the Class}}{\text{Total Number of Wells in the Study Area}}}{\frac{\text{Number of Pixels in the Class} - \text{Number of Wells in the Class}}{\text{Number of Pixels in the Study Area} - \text{Total Number of Wells in the Study Area}}} \right] \quad (3)$$

where P_p is the prior probability of groundwater occurrence which was computed as:

$$P_p = \frac{\text{Total Number of Wells in the Study Area}}{\text{Total Number of Pixels in the Study Area}} \quad (5)$$

Step 6: calculation of WOE probability (P) for each class of a theme. The WOE probabilities of individual classes of different themes were calculated as:

$$P = \exp \left\{ \sum W^+ + \ln P_p \right\} \quad (4)$$

Step 7: preparation of a groundwater prospect map of the study area based on the range of WOE probability values over the study area.

Step 8: validation of the prepared groundwater prospect map using testing wells.

Fig. 6 Mean groundwater fluctuation map of the study area

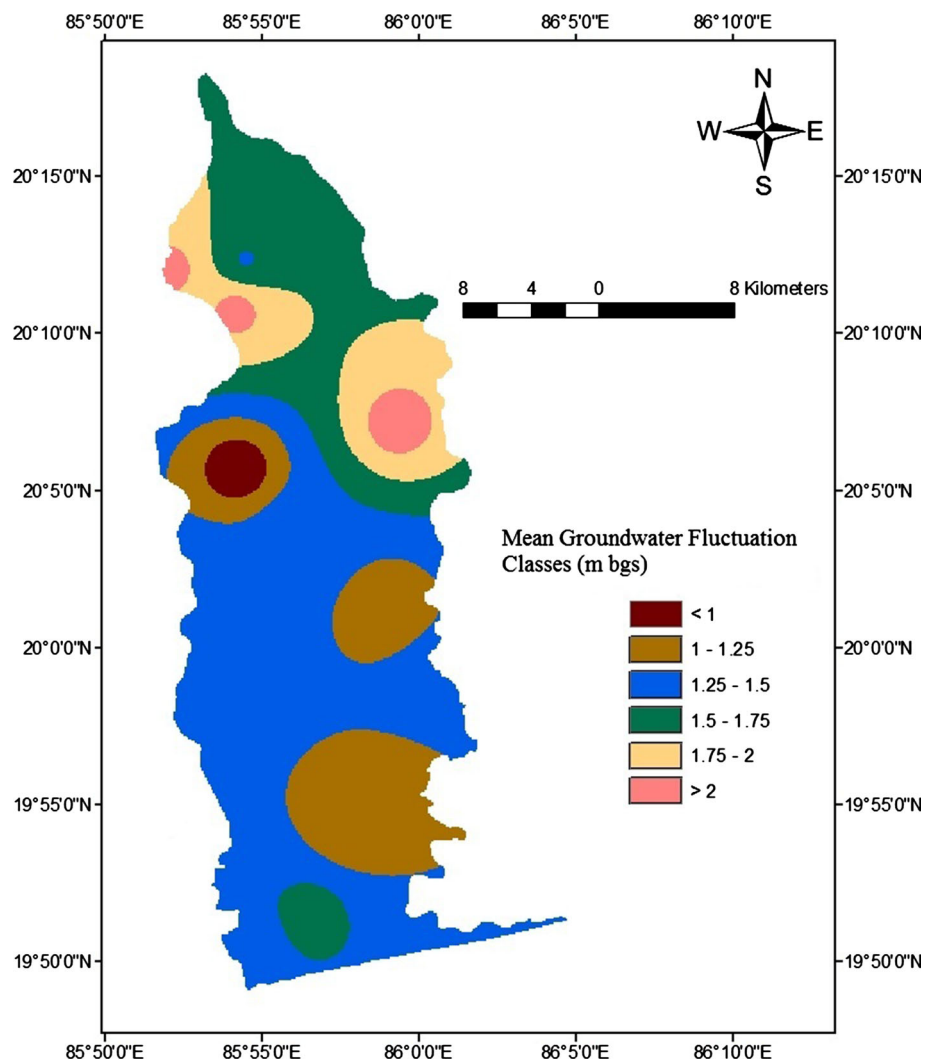
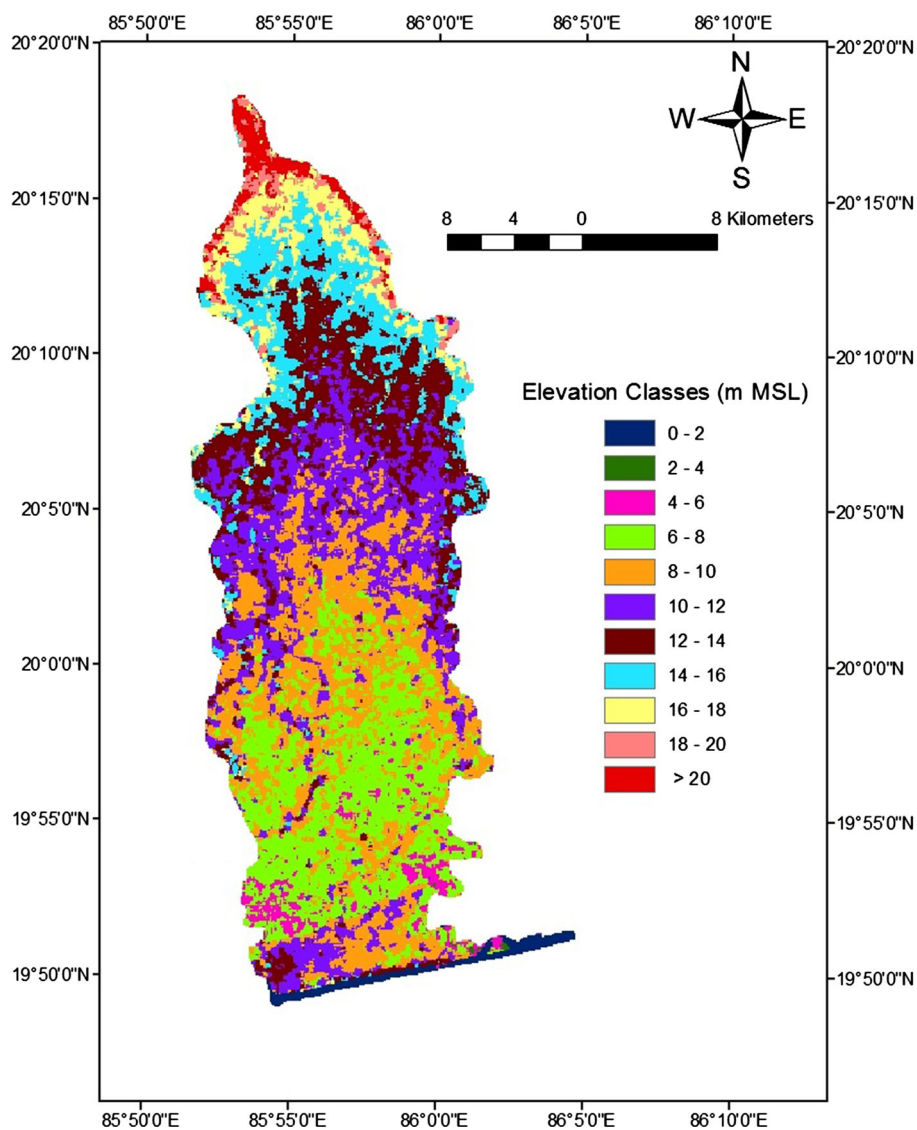


Fig. 7 Elevation map of the study area



Evaluation of groundwater prospect mapping methods

Finally, a comparative evaluation of the two approaches used for groundwater prospect mapping was performed on the basis of prediction accuracy calculated by comparing the groundwater prospect maps generated by the two approaches with the map of well yields.

Results and discussion

Groundwater characteristics of the study area

The variation of post-monsoon groundwater depths (mean of 1997–2011) over the study area is shown in Fig. 4. It reveals that the mean post-monsoon groundwater depth in the area ranges from 0.95 to 3.65 m below the ground surface (bgs). Similarly, Fig. 5 depicts the variation of

mean pre-monsoon groundwater depths over the study area. Obviously, the mean pre-monsoon groundwater depth in the study area varies from 1.75 to 5.6 m below the ground surface. Moreover, the mean seasonal groundwater fluctuation ranges from 0.78 to 2.15 m (Fig. 6), with a major portion of the study area having a mean groundwater fluctuation of 1.25–1.5 m. Thus, the significant seasonal groundwater fluctuations in the study area indicate appreciable recharge to the aquifer during the monsoon season (wet period). It is recommended that future study should focus on the determination of safe yield/sustainable yield of the aquifer(s) underlying the study area.

Characterization of the thematic layers

The thematic layers or themes are characterized by classifying their features into suitable groups that can help

Fig. 8 Slope map of the study area

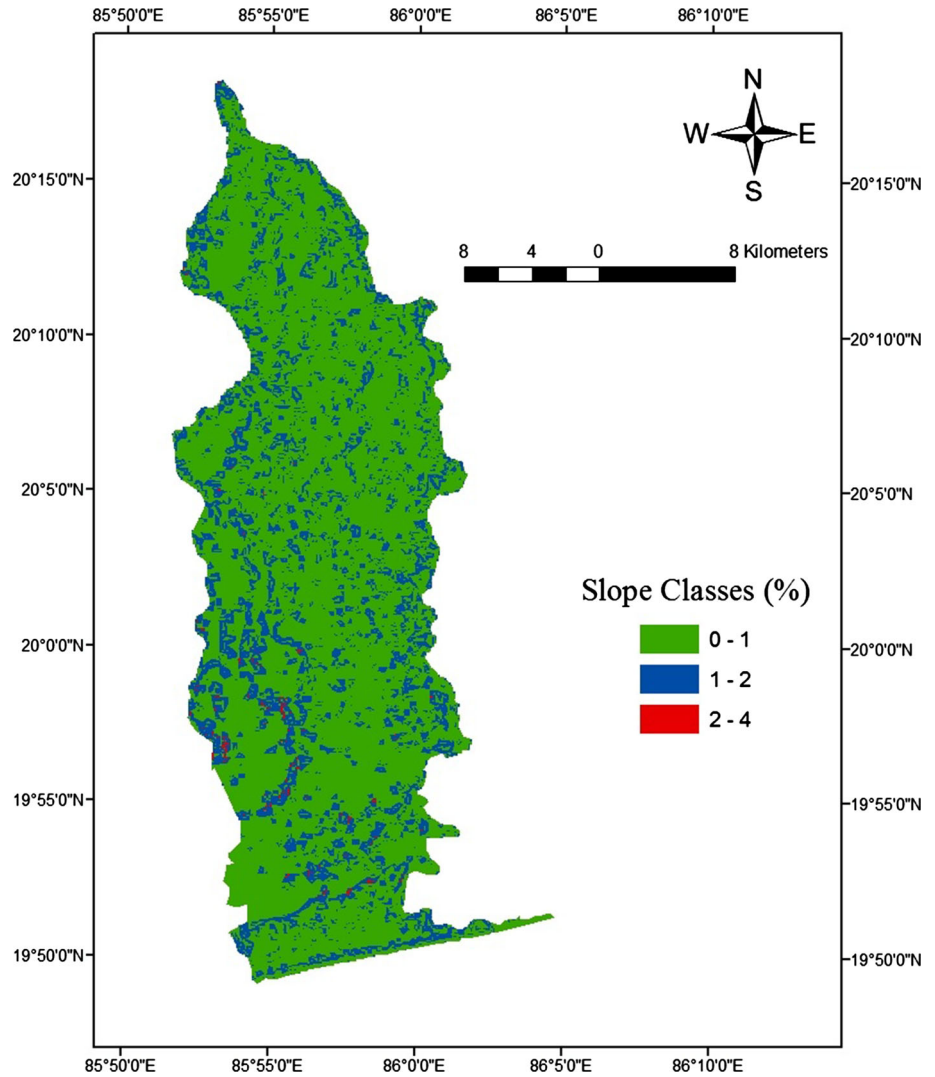


Table 3 Slope statistics of the study area

Sl. no.	Slope class (%)	Area covered (km ²)	Area covered (%)
1	0–1	490	78.84
2	1–2	128	20.64
3	2–4	2	0.32

interpret their importance in groundwater occurrence. The features of the six selected layers are described in the subsequent sub-sections.

Features of topographic elevation layer

The topographic elevation map of the study area is shown in Fig. 7, which indicates almost flat topography over the study area, with the elevation varying from 0 to 26 m MSL. Thus, on the basis of topographic elevation, the study area can be divided into 11 classes as illustrated in Fig. 7.

Features of slope layer

The prevailing slope in the study area varies from 0 to 4 % (Fig. 8). The slope statistics of the study area are presented in Table 3, which reveals that a major portion of the study area (nearly 79 %) falls under the 0–1 % slope category. This slope class can be considered as ‘very good’ for groundwater occurrence due to nearly flat terrain and hence relatively high infiltration potential. The area having 1–2 % slope can be considered as ‘good’ from groundwater viewpoint due to slightly undulating topography with some runoff. On the other hand, the area having a slope of 2–4 % is likely to produce relatively high runoff and low infiltration and hence can be categorized as ‘moderate’.

Features of geology layer

The statistics and map of geology of the study area are presented in Table 4 and Fig. 9, respectively, which

indicate two types of geology features, viz., alluvium and laterite. A major portion of the study area (434 km²) is covered by laterite formation which encompasses about 61 % of the total area and is found in the middle and southern portions of the study area. Laterite is somewhat a porous rock formation, which can form potential aquifers along topographic lows and moderate groundwater potential can be expected in this area. Further, about 39 % of the study area (i.e., 186 km²) is occupied by alluvium formation. Alluvium constitutes a very good water-bearing formation and is

supposed to be an important source of groundwater in the deltaic regions.

Features of land use/land cover layer

Land use/land cover plays an important role in deciding the extent of infiltration rate and recharge rate. In the study area, six major land use/land cover categories, namely agricultural land, dense forest, degraded forest, wasteland, settlements, and rivers and water bodies are found (Table 5). The spatial distribution of land use/land cover in the study area is illustrated in Fig. 10.

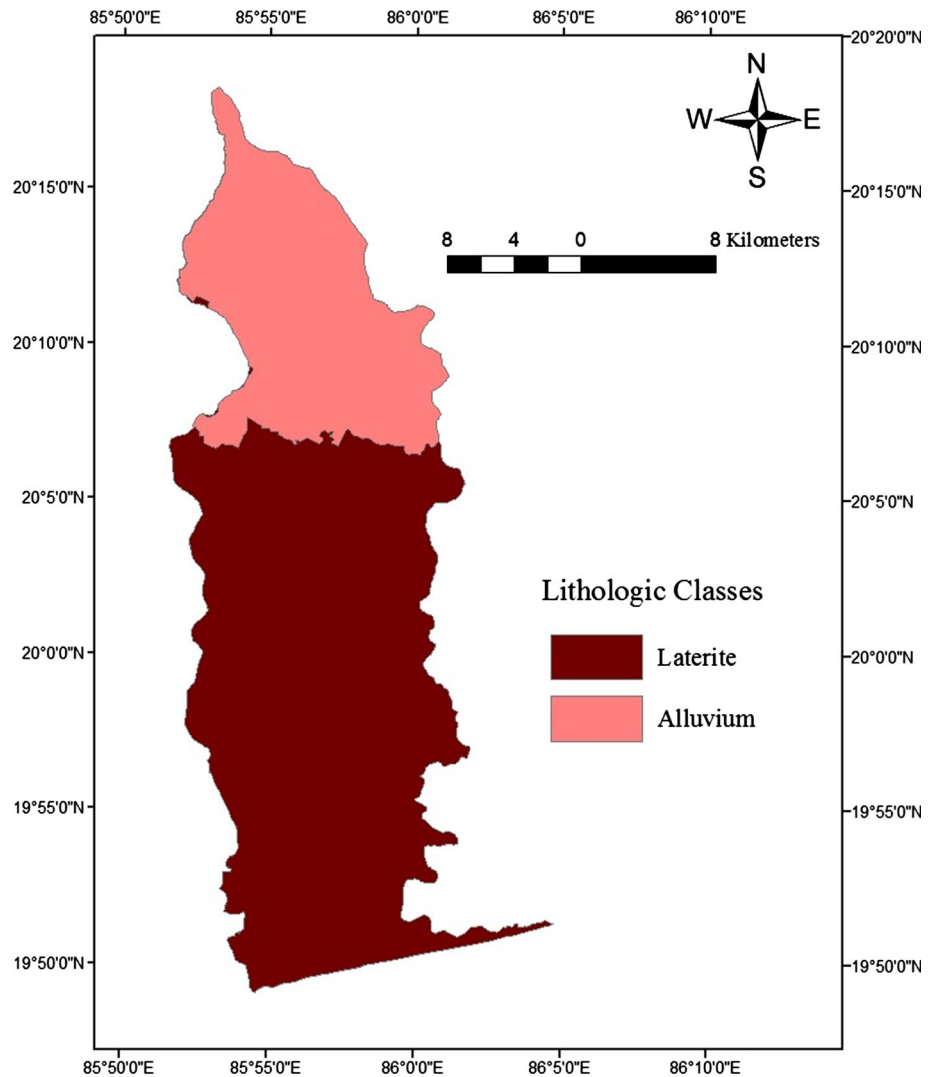
Features of soil layer

The soil map showing the variation of soil types in the study area is shown in Fig. 11 and the soil statistics are presented in Table 6. The soil classes found in the study

Table 4 Geology statistics of the study area

Sl. no.	Geology class	Area covered (km ²)	Area covered (%)
1	Laterite	434	61
2	Alluvium	186	39

Fig. 9 Geology map of the study area



area are: silty loam, clayey loam, coarse sand, very fine sand and sandy loam. According to their hydraulic characteristics, these soil classes can be considered as ‘very

good’, ‘good’, ‘moderate’ and ‘poor’ depending on their contribution to groundwater recharge.

Features of drainage density layer

The density of surface drainage indirectly indicates groundwater potential of an area due to its relation with surface runoff and permeability, and hence it is considered as one of the hydrological indicators of groundwater occurrence in the study area. Drainage density map of the study area was prepared on the micro-watershed basis and reveals that the drainage density ranges from 0 to 2.8 km/km² (Fig. 12). Based on the drainage density of the micro-watersheds, the drainage density was grouped into five classes, the statistics of which are presented in Table 7. It is

Table 5 Land use/land cover statistics of the study area

Sl. no.	Land use/land cover class	Area covered (km ²)	Area covered (%)
1	Agricultural land	504	81.4
2	Dense forest	18	2.9
3	Degraded forest	1	0.2
4	Wasteland	11	1.8
5	Settlements	76	12.3
6	Rivers and water bodies	9	1.4

Fig. 10 Land use/land cover map of the study area

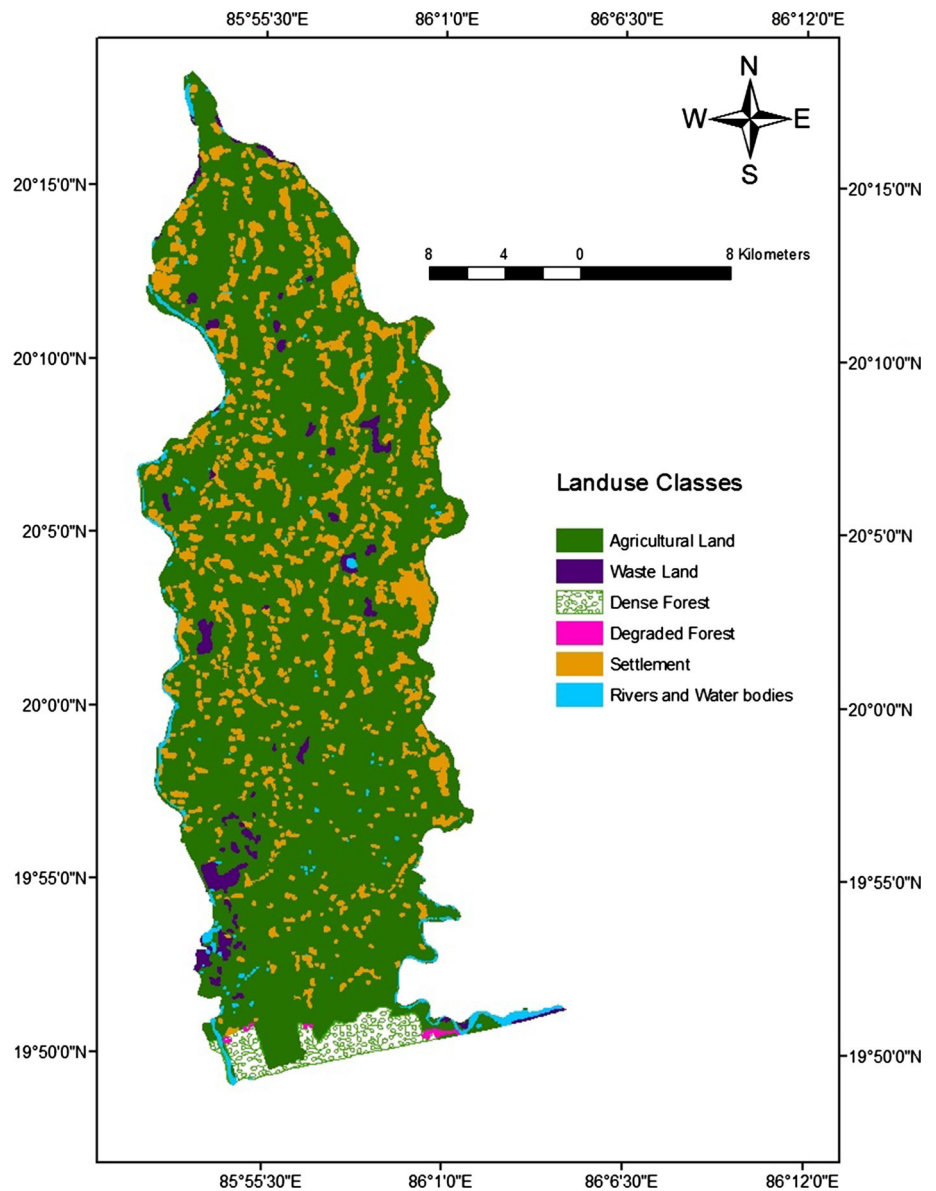
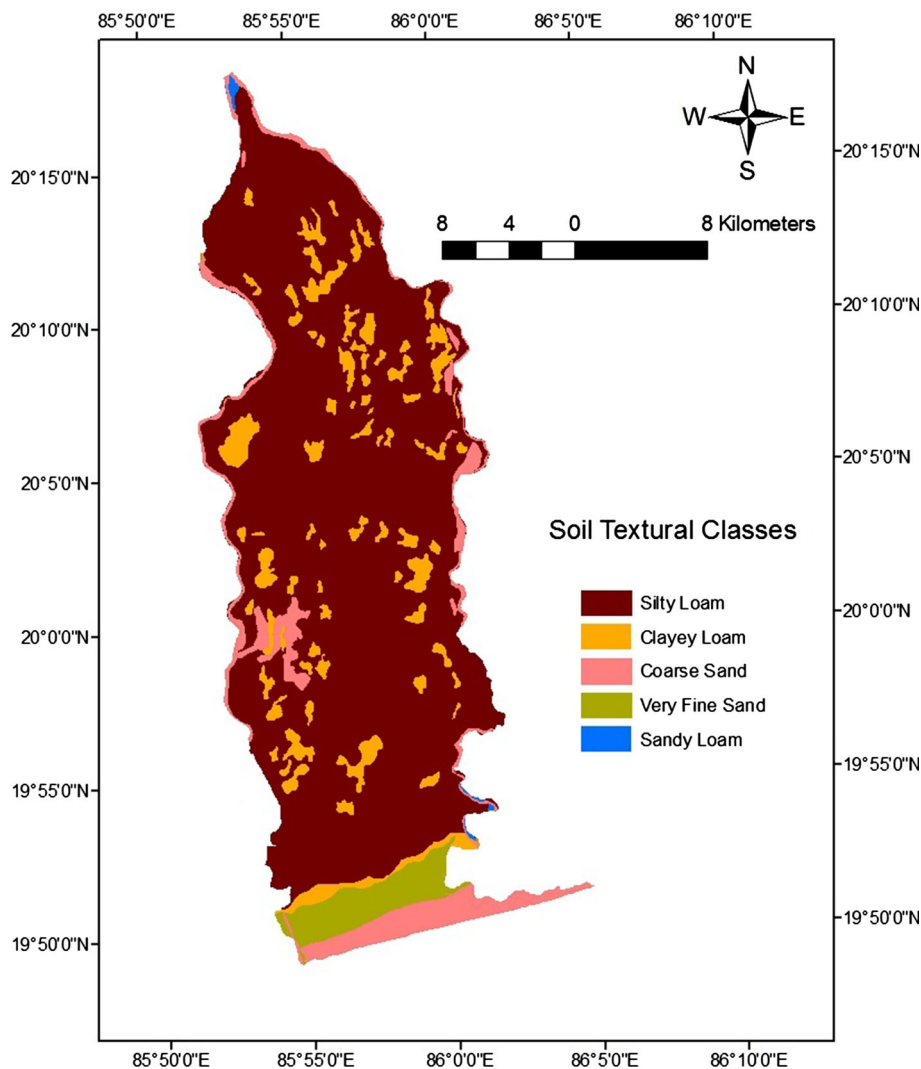


Fig. 11 Soil map of the study area**Table 6** Variation of soil types in the study area

Sl. no.	Soil class	Area covered (km ²)	Area covered (%)
1	Silty loam	489	78.87
2	Clayey loam	60	9.67
3	Coarse sand	46	7.43
4	Very fine sand	24	3.87
5	Sandy loam	1	0.16

apparent that a major portion of the study area (nearly 88 %) falls under 0–0.50 km/km² drainage density category, which can be considered as ‘very good’ for groundwater occurrence. Similarly, the remaining drainage density classes such as 0.50–0.75 km/km² can be considered as ‘good’, 0.75–1 km/km² as ‘moderate’ and >1 km/km² can be considered as ‘poor’ from the viewpoint of groundwater potential.

Groundwater prospect maps of the study area

Groundwater prospect map based on Approach I

In this approach, RS, GIS and AHP techniques are integrated for identifying and delineating groundwater prospect zones. The weights were assigned to all the thematic layers using Saaty’s AHP scale as shown in Table 8. Normalized weights derived from the pairwise comparison matrix are presented in Table 9. Similarly, the weights assigned to all the features of individual themes were normalized and are presented in Table 10. The CR of the pairwise comparison matrix for all the thematic layers was found to be 0.00324, i.e., less than the threshold limit of 0.10 which indicates that the weights assigned to the thematic layers are consistent. The weights assigned to different features of individual thematic layer were also found to be consistent (CR < 0.10).

Fig. 12 Drainage density map of the study area

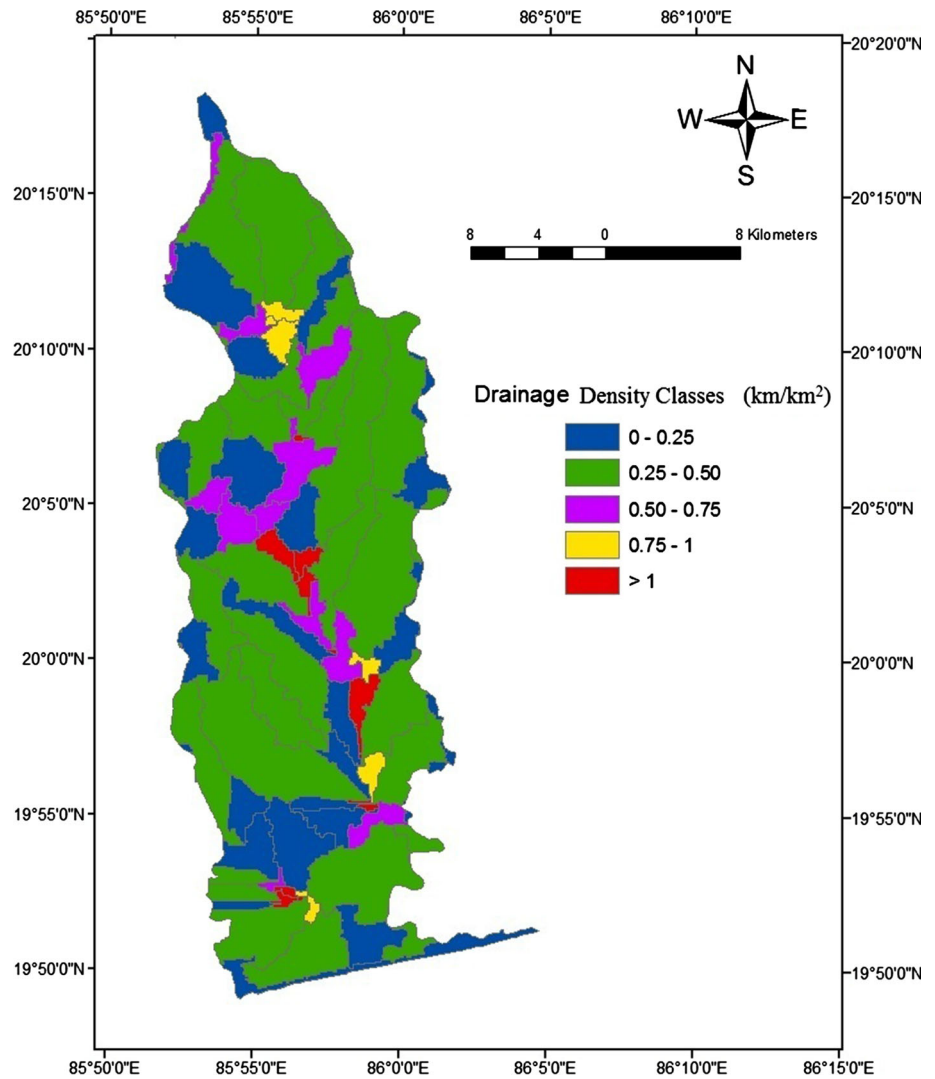


Table 7 Drainage density statistics of the study area

Sl. no.	Drainage density class (km/km ²)	Area covered (km ²)	Area covered (%)
1	0–0.25	152	24.5
2	0.25–0.50	395	63.7
3	0.50–0.75	47	7.6
4	0.75–1	13	2.1
5	>1	13	2.1

Table 8 Weights of the five thematic layers for groundwater prospect zoning using Saaty’s AHP scale

Sl. no.	Theme	Groundwater prospect	Assigned weight
1	Geology	Very good	7
2	Soil	Good	5
3	Land use/land cover	Good	4.5
4	Drainage density (km/km ²)	Moderate	4
5	Slope (%)	Moderate	4

The normalized weights of the five thematic layers and their features were aggregated and GWPI was computed in the GIS environment. Finally, a groundwater prospect map of the study area was generated by dividing the study area into four distinct zones based on the GWPI values, i.e., ‘very good’ (GWPI = 0.33–0.40), ‘good’ (GWPI = 0.29–0.33), ‘moderate’ (GWPI = 0.25–0.29) and ‘poor’ (GWPI = 0.04–0.25) as shown in Fig. 13.

It is apparent from Fig. 13 that the groundwater prospect in the northern and southern coastal parts of the study area can be categorized as ‘very good’ and ‘good’. In other words, these portions of the study area have quite favorable hydrological/hydrogeological conditions for groundwater storage and hence these areas are expected to be rich in groundwater.

Table 9 Pairwise comparison matrix and normalized weights of the five thematic layers

	Thematic layers					Geometric mean	Normalized weight
	GG	Soil	LULC	Slope	DD		
GG	7/7	7/5	7/4.5	7/4	7/4	1.461	0.286
Soil	5/7	5/5	5/4.5	5/4	5/4	1.044	0.204
LULC	4.5/7	4.5/5	4.5/4.5	4.5/4	4.5/4	0.939	0.184
Slope	4/7	4/5	4/4.5	4/4	4/4	0.835	0.163
DD	4/7	4/5	4/4.5	4/4	4/4	0.835	0.163
Column total =						5.115	1

GG geology, LULC land use/land cover, DD drainage density

Table 10 Normalized weights of the five thematic layers and their features

Theme	Normalized weight of themes	Features of theme	Groundwater prospect	Assigned weight	Normalized weight of features	Total weight
Geology	0.286	Alluvium	Good	8	0.61	0.1744
		Laterite	Moderate	5	0.39	0.1115
Soil	0.204	Coarse sand	Very good	8	0.33	0.0673
		Sandy loam	Good	7	0.29	0.0591
		Very fine sand	Moderate	6	0.25	0.0510
		Silty loam	Poor	2	0.08	0.0163
		Clayey loam	Very poor	1	0.04	0.0082
Land use/land cover	0.184	Rivers and water bodies	Very good	7	0.26	0.0478
		Agricultural land	Good	6	0.22	0.0404
		Dense forest	Moderate	5	0.18	0.0331
		Degraded forest	Moderate	4	0.15	0.0276
		Wasteland	Poor	3	0.11	0.0202
		Settlements	Very poor	2	0.08	0.0147
Drainage density (km/km ²)	0.163	0–0.25	Very good	6	0.29	0.0472
		0.25–0.50	Very good	5.5	0.26	0.0423
		0.50–0.75	Good	5	0.24	0.0391
		0.75–1	Moderate	3	0.14	0.0228
		>1	Poor	1.5	0.07	0.0114
Slope (%)	0.163	0–1	Very good	7	0.39	0.0635
		1–2	Good	6	0.33	0.0537
		2–4	Moderate	5	0.28	0.0456

Groundwater prospect statistics of the study area based on Approach I are presented in Table 11, which reveals that the area covered by ‘very good’ and ‘good’ groundwater prospect zones is about 240.74 km² ($\approx 39\%$) and these zones are dominated in the northern and southern portions of the study area. The ‘moderate’ groundwater prospect zone is prevalent in the central and southern portions of the study area and encompasses an area of nearly 313.3 km², which is about 51 % of the total study area. The hydrogeomorphic feature available in this portion of the study area is laterite type of geology, which also suggests moderate capacity of groundwater storage. ‘Poor’ groundwater prospect zone covers an area of 64.54 km² (about 10 %) and is distributed in scattered patches in the central and southern portions of the study area.

Groundwater prospect maps based on Approach II

The groundwater prospect maps prepared by using two probabilistic models, viz., FR and WOE, are presented below with the help of examples. The number of wells and the number of pixels present in individual features of a factor (thematic layer) are summarized in Table 12.

1. Frequency ratio modeling results

The calculation of FR for the alluvium feature of the ‘geology’ factor is presented below as an example:

number of wells present in the alluvium feature of the geology factor = 23,
total number of wells in the study area = 55,

Fig. 13 Groundwater prospect map of the study area based on Approach I

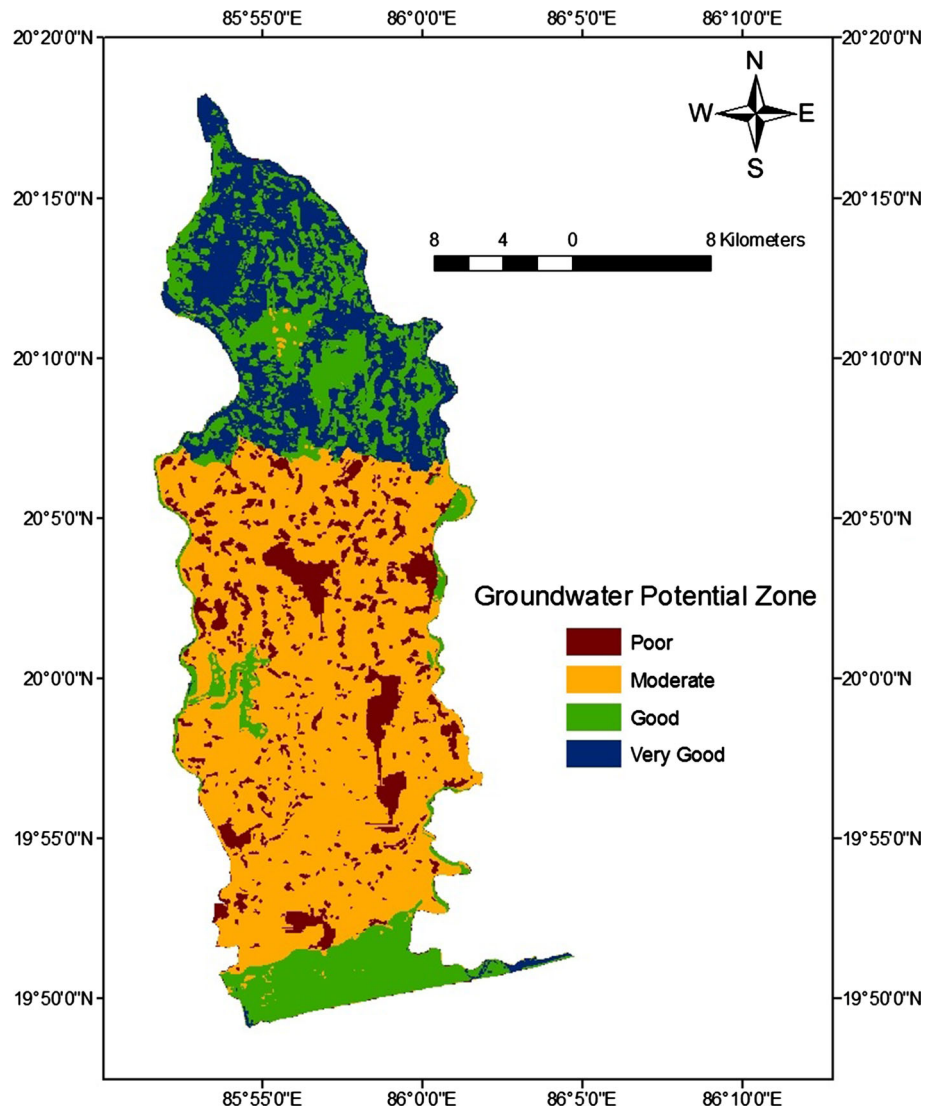


Table 11 Groundwater potential statistics of the study area based on Approach I

Groundwater prospect	Area (km ²)	Percentage area	Range of GWPI values
Poor	64.54	10.34	0.04–0.25
Moderate	313.30	50.70	0.25–0.29
Good	136.53	22.10	0.29–0.33
Very good	104.21	16.86	0.33–0.40

number of pixels in the alluvium feature of the geology factor = 203,858,
 total number of pixels in the geology factor = 685,829,
 percentage of wells for the alluvium feature of the geology factor = $(23/55) \times 100 = 41.8$ and
 percentage of area for the alluvium feature of the geology factor = $(203,858/685,829) \times 100 = 29.7$.

Therefore, FR for the alluvium feature of the geology factor is $41.8 \div 29.7 = 1.407$.

Similarly, FR for each feature of the thematic layers was calculated as shown in Table 13. The GWPI obtained from the FR values provided a basis for identifying groundwater prospect zones. Based on the GWPI values, a groundwater prospect map of the study area was generated by dividing the study area into four distinct zones: ‘poor’ (GWPI = 0–3.92), ‘moderate’ (GWPI = 3.92–5.05), ‘good’ (GWPI = 5.05–6.47) and ‘very good’ (GWPI = 6.47–12.48) as shown in Fig. 14. Groundwater potential statistics of the study area as obtained from the FR model are presented in Table 14.

It is discernible from Fig. 14 that the groundwater potential zones ‘very good’ and ‘good’ occur mainly in the northern part and in some patches scattered over the study area. The area covered by ‘very good’ and ‘good’

Table 12 Number of pixels and number of wells in the individual features of the factors affecting groundwater

Factor	Features of factor	No of pixels (30 × 30 m)	No. of wells
Geology	Alluvium	203,858	23
	Laterite	481,971	32
	Total	685,829	55
Soil	Coarse sand	50,881	2
	Sandy loam	1361	0
	Very fine sand	26,634	0
	Silty loam	540,580	49
	Clayey loam	66,373	4
	Total	685,829	55
	Land use/land cover	Rivers and water bodies	9490
Agricultural land		559,421	40
Dense forest		19,699	0
Degraded forest		759	0
Wasteland		12,173	0
Settlements		84,287	15
Total		685,829	55
Drainage density (km/km ²)		0–0.25	168,801
	0.25–0.50	438,470	34
	0.50–0.75	52,164	6
	0.75–1	11,958	6
	>1	14,436	1
Total	685,829	55	
Slope (%)	0–1	540,707	39
	1–2	142,240	16
	2–4	2882	0
	–	685,829	55

groundwater potential zone is about 236 km² (38 %), while the ‘moderate’ groundwater potential zone encompasses an area of 322 km², which is 52 % of the total study area (Table 14). Thus, the ‘moderate’ groundwater potential zone is dominating in the study area. Further, the southern part and scattered small patches in the central portions fall in the ‘poor’ groundwater potential zone that covers an area of 63 km² (10.2 %).

2. Weight of evidence modeling results

As an example, the calculation of WOE (W^+) and WOE probability (P) for the alluvial feature of the geology factor is illustrated below:

number of wells present in the alluvium feature of the geology factor = 23,
total number of wells in the study area = 55,
number of pixels in the alluvium feature of the geology factor = 203,858, and

total number of pixels in the geology factor = 685,829.
Therefore,

$$W^+ = \ln \frac{23/55}{(203858 - 23)/(685829 - 55)} = 0.3414,$$

$$P_p = 55 \div 685,829 = 0.00008019 \text{ and}$$

$$P = \exp \{0.3414 + \ln (0.00008019)\} = 0.0001128.$$

Similarly, the WOE (W^+) and WOE probability (P) for each feature of the five thematic layers (factors) were calculated as summarized in Table 13. Finally, a groundwater prospect map of the study area was generated by dividing the study area into four distinct zones based on the WOE probability values, i.e., ‘poor’ (GWPI = 0–0.00168), ‘moderate’ (GWPI = 0.00169–0.00275), ‘good’ (GWPI = 0.00276–0.00526) and ‘very good’ (GWPI = 0.00526–0.00786). The map showing various groundwater potential zones of the study area as obtained from the WOE model is shown in Fig. 15. It can be seen from Fig. 15 that the groundwater potential in the northern portion and some parts of the central portion of the study area fall under ‘good’ groundwater potential zone, but the ‘very good’ groundwater potential zones occur in a couple of patches in the northern, central and southern parts of the study area. The area covered by ‘very good’ and ‘good’ groundwater potential zone is about 44.4 % (Table 15). The central portion, some part of the southern portion and some patches in the northern portion of the study area fall under ‘moderate’ groundwater potential zone, which constitute 48 % of the total study area. The lower southern part and a few small patches/strips in the central and northern parts of the study area have ‘poor’ groundwater potential encompassing an area of 7.6 % (Table 15).

Efficacy of the multicriteria decision analysis and probabilistic modeling

Prediction accuracy of Approach I

The verification of Approach I using measured well yields of 77 tubewells reveals that 30 ‘high-discharge’ (>100 m³/h) wells out of 40 exist in the ‘good’ and ‘very good’ zones, and out of the remaining 10 wells, 7 exist in the ‘moderate’ zone and 3 in the ‘poor’ zone. Furthermore, 4 out of 34 ‘medium-discharge’ (60–100 m³/h) wells fall in the ‘good’ zone, 28 in the ‘moderate’ zone and the remaining 2 in the ‘poor’ zone. Based on these findings, the prediction accuracy of Approach I is 76.62 %; its calculation is given below:

total number of tube wells = 77,
number of tube wells where there is an agreement between the expected and the actual yield = 59 and

Table 13 Frequency ratio (FR), weight of evidence (W^+) and WOE probability (P) for the five factors

Factors	Features of factor	Area (%)	Well (%)	FR	W^+	P
Geology	Alluvium	29.7	0.418	1.407	0.3414	0.0001128
	Laterite	70.3	0.582	0.827	-1.8882	0.0000121
Soil	Coarse sand	7.40	3.63	0.490	-0.7131	0.0000393
	Sandy loam	0.30	0	0	0.0000	0.0000802
	Very fine sand	3.80	0	0	0.0000	0.0000802
	Silty loam	78.80	89.10	1.130	0.1226	0.0000906
	Clayey loam	9.70	7.27	0.749	-0.1909	0.0000662
Land use/land cover	Rivers and water bodies	1.38	0	0	0.0000	0.0000802
	Agricultural land	81.57	72.73	0.89	-0.1146	0.0000715
	Dense forest	2.87	0	0	0.0000	0.0000802
	Degraded forest	0.12	0	0	0.0000	0.0000802
	Wasteland	1.77	0	0	0.0000	0.0000802
Drainage density (km/km ²)	Settlements	12.29	27.27	2.21	0.7978	0.0001780
	0–0.25	24.5	14.54	0.593	-0.5286	0.0000472
	0.25–0.50	63.7	61.82	0.970	-0.0336	0.0000775
	0.50–0.75	7.6	10.91	1.435	0.361	0.0001152
	0.75–1	2.1	10.91	5.455	1.8357	0.0005027
Slope (%)	>1	2.1	1.82	0.866	-0.1466	0.0000692
	0–1	78.84	70.91	0.899	-0.1104	0.0000718
	1–2	20.74	29.09	1.403	0.3549	0.0001143
	2–4	0.42	0	0	0.0000	0.0000802

number of tube wells where there is a disagreement between the expected and the actual yield = 18.

Therefore, the prediction accuracy of Approach I = $59 \div 77 = 76.62\%$.

Prediction accuracy of Approach II

The verification of Approach II was performed using measured well yields of 22 testing tube wells in the study area. The verification of the groundwater prospect map based on the FR model reveals that five out of eight ‘high-discharge’ wells exist in the ‘good’ zone, two in the ‘moderate’ zone and one in the ‘poor’ zone. However, 2 out of 11 ‘medium-discharge’ wells exist in the ‘good’ zone, 8 in the ‘moderate’ zone and 1 in the ‘poor’ zone. Based on these findings, the prediction accuracy of the FR model is 68.18 % as computed below:

total number of testing tube wells = 22,
 number of tube wells where there is an agreement between the expected and the actual yield = 15 and
 number of tube wells where there is a disagreement between the expected and the actual yield = 7.
 Therefore, the prediction accuracy of the FR model = $15 \div 22 = 68.18\%$.

On the other hand, the verification of the groundwater prospect map based on the WOE model reveals that six out

of eight ‘high-discharge’ wells exist in the ‘good’ zone and two in the ‘moderate’ zone. However, 2 out of 11 ‘medium-discharge’ wells exist in the ‘good’ zone, eight in the ‘moderate’ zone and one in the ‘poor’ zone. Based on these findings, the prediction accuracy of the WOE model is 72.72 % as estimated below:

total number of testing tube wells = 22,
 number of tube wells where there is an agreement between the expected and the actual yield = 16 and
 number of tube wells where there is a disagreement between the expected and the actual yield = 6.
 Therefore, the prediction accuracy of the WOE model = $16 \div 22 = 72.72\%$.

It is clear from the above verification results that although the results of both the approaches are satisfactory, Approach I is much superior to Approach II (both WOE and FR models). Among the two probabilistic models used for groundwater prospect mapping, the prediction accuracy of the WOE model is higher than that of the FR model.

Spatial prediction of groundwater prospect: comparative evaluation

A comparison of the areas under the four identified zones ‘very good’, ‘good’, ‘moderate’ and ‘poor’ as predicted by the three methods (AHP, FR and WOE) is illustrated in

Fig. 14 Groundwater prospect map of the study area based on the FR model

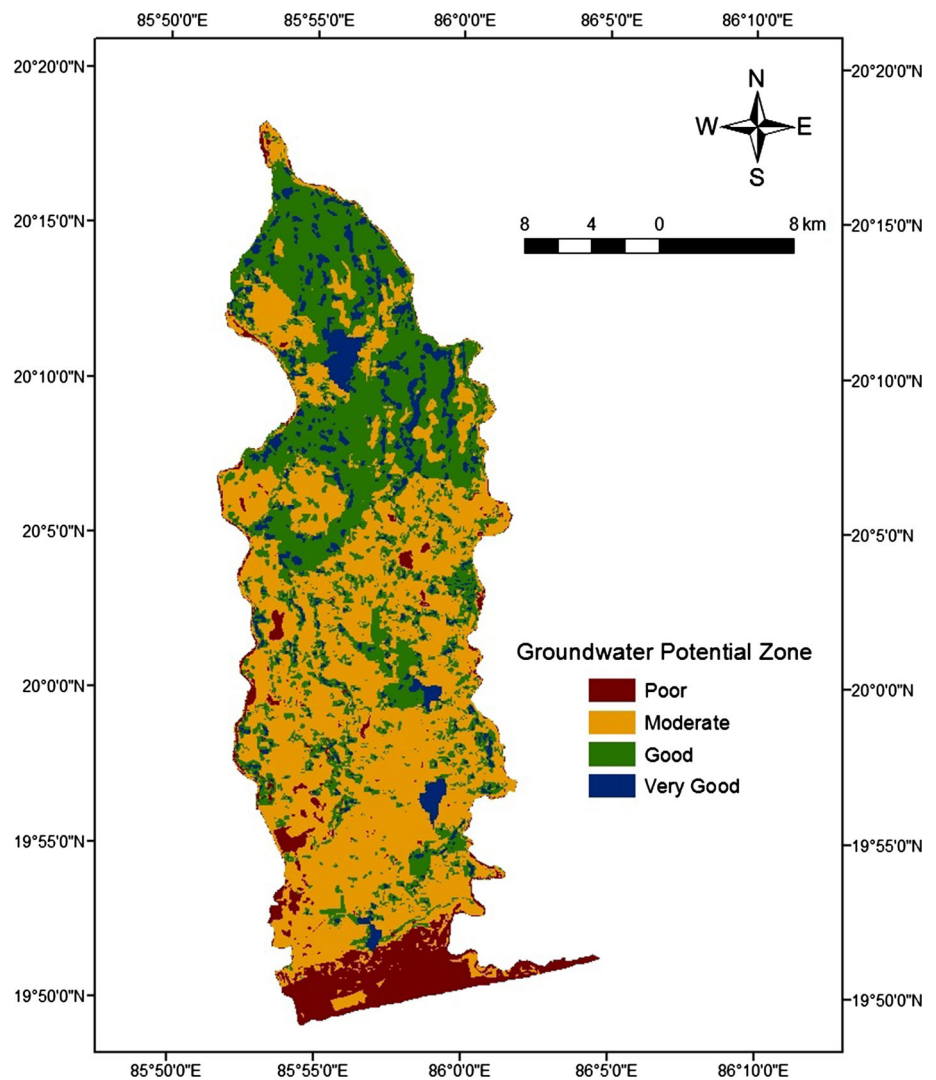


Table 14 Groundwater potential statistics of the study area based on the FR model

Groundwater prospect	Area (km ²)	Percentage area	Range of GWPI values
Poor	63	10.2	0–3.92
Moderate	322	52	3.92–5.05
Good	192	31	5.05–6.47
Very good	44	7	6.47–12.48

Fig. 16. It is evident from this figure that the total areas under ‘moderate’ and ‘poor’ zones predicted by the FR model are more or less the same as those predicted by the AHP technique; differences in the areas vary from 2.78 to 2.39 %, respectively, with respect to the AHP technique. However, the total area under ‘very good’ zone is under-predicted (57.78 %) and that under ‘good’ zone is over-predicted (40.63 %) by the FR model as compared to the AHP technique (Fig. 16). In contrast, the spatial

distribution of the zones over the study area as predicted by the FR model varies appreciably, with a high level of disagreement with the spatial distribution of the zones predicted by the AHP technique (Figs. 13, 14). The ‘moderate’ groundwater prospect zone as predicted by the FR model and AHP technique is dominant and located in the central and southern portions of the study area. However, the major discrepancy in the spatial prediction by these two techniques is found in the southernmost part of the study area. This is because of the absence of pumping wells in the southernmost portion of the study area (Fig. 3) which provides the basic criteria for FR modeling.

On the other hand, the spatial distribution of the zones predicted by the WOE model matches with that predicted by the AHP technique to a greater extent as revealed by Table 16, Figs. 13 and 15. A major difference in the spatial prediction is found only in the southernmost portion of the study area due to the absence of pumping wells in this region. It should be noted that the presence/absence of

Fig. 15 Groundwater prospect map of the study area based on the WOE model

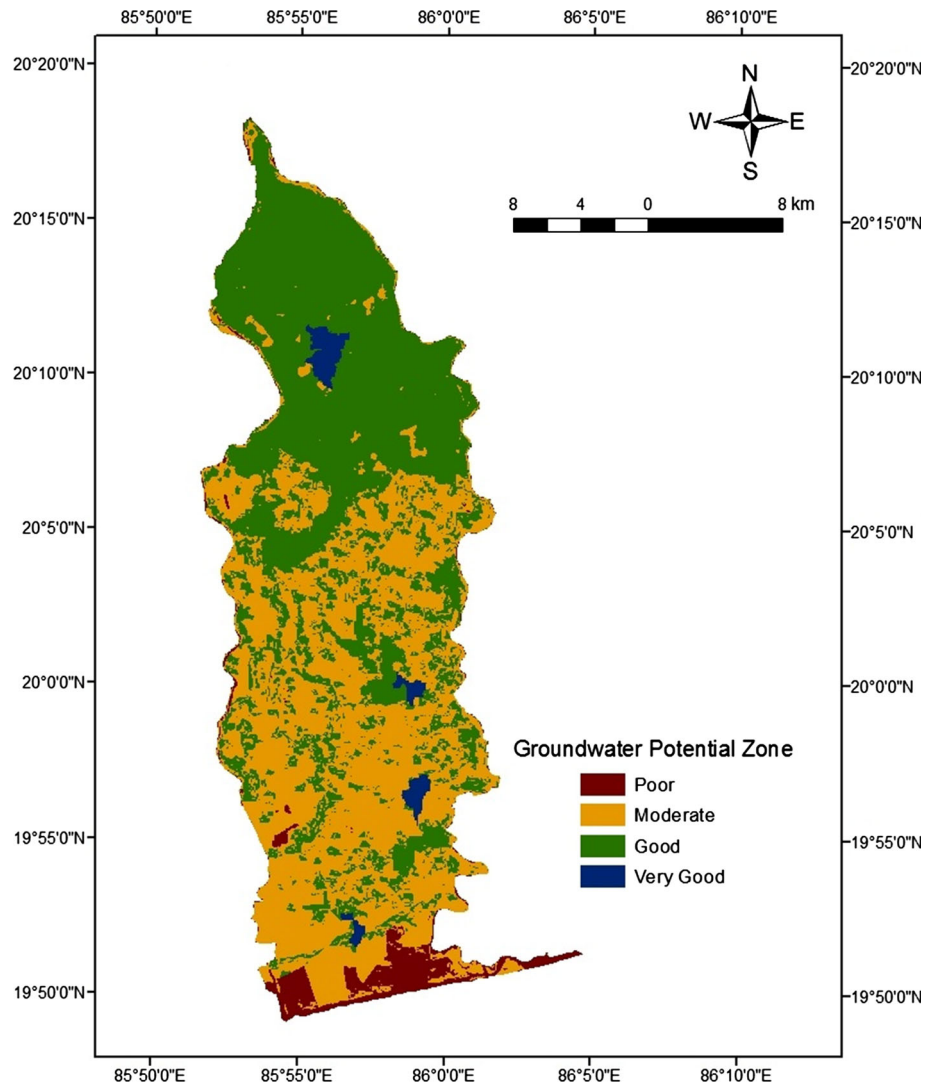


Table 15 Groundwater potential statistics of the study area based on the WOE model

Groundwater prospect	Area (km ²)	Percentage area	Range of GWPI values
Poor	47	7.6	0–0.00168
Moderate	297	48	0.00169–0.00275
Good	254	41	0.00276–0.00526
Very good	21	3.4	0.00526–0.00786

pumping wells provides the basic criteria for WOE modeling, whereas AHP technique is dependent on only hydrologic/hydrogeologic factors. As a result, the AHP technique predicts good/very good potential of groundwater because of favorable hydrologic/hydrogeologic factors in the southernmost portion, while the WOE model predicts moderate and poor potential of groundwater in this portion. Furthermore, for the WOE model, the total area under ‘poor’ zone differs by 27.18 % as compared to the AHP

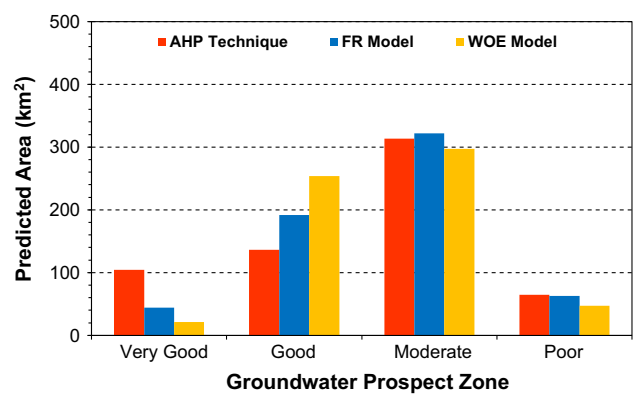


Fig. 16 Area under different groundwater potential zones predicted by the AHP, FR and WOE techniques

technique, while the total area under ‘moderate’ potential zone differs by 5.2 %. Similarly, the differences in the total areas under ‘very good’ and ‘good’ potential zones vary

Table 16 Comparison of spatial prediction of different groundwater prospect zones by the AHP, WOE and FR techniques

Techniques	Spatial prediction of groundwater prospect by the three techniques						
	Northern portion	North-east portion	North-west portion	Central portion	South-east portion	South-west portion	Southern portion
1. AHP	Very good or good zones	Very good or good zones	Very good or good zones	Moderate zone with few patches of poor and good zones	Moderate zone with few patches of poor and good zones	Moderate zone with few patches of poor and good zones	Moderate and good zones with few patches of very good and poor zones
2. WOE	Good zone with patches of moderate and very good zones	Good zone with few patches of moderate zone	Good zone with few patches of moderate zone	Moderate and good zones with few patches of very good zone	Moderate zone with patches of good and very good zones	Moderate zone with patches of good and poor zones	Moderate and poor zones with patches of good and very good zones
3. FR	Good zone with patches of very good and moderate zones and few patches of poor zone	Good zone with patches of very good and moderate zones	Moderate zone with patches of good, very good and poor zones	Moderate zone with patches of good, very good and poor zones	Moderate zone with patches of good and very good zones	Moderate zone with few patches of good and poor zones	Poor zone with few patches of moderate, good and very good zones

from 79.85 to 86.04 %, respectively, with respect to the AHP technique (Fig. 16).

Thus, the findings of the comparative evaluation of spatial distribution of groundwater prospect zones are in agreement with the results of prediction accuracy of the probabilistic models, i.e., the reliability of AHP technique is greater than the probabilistic models (FR and WOE). Among the probabilistic models, the performance of the WOE model is superior to that of the FR model. Therefore, the AHP technique is strongly recommended for better identification and delineation of groundwater prospect zones in the study area. The WOE model can serve as an alternative technique for the study area. However, considering the basic requirement of adequate data on number of pumping wells over a basin/sub-basin for the WOE model, the practical applicability of this model is limited, especially in data-scarce countries.

Conclusions

The present study deals with the evaluation of the efficacy of two approaches for spatial prediction of groundwater prospect through a case study. Five significant thematic layers related to groundwater occurrence in the study area were considered for both the approaches. The first approach includes integrated use of RS, GIS and multicriteria decision analysis (AHP), whereas the second approach includes GIS-based probabilistic modeling using FR and WOE models. The analysis of the spatial modeling results of the two approaches indicated that the groundwater prospect map obtained by Approach I (AHP technique) demarcated the study area with the ‘very good’ zone encompassing about 17 % of the study area, ‘good’ zone 22 %, ‘moderate’ zone 51 % and the ‘poor’ groundwater prospect zone covering about 10 % of the study area. On the other hand, the groundwater prospect map obtained by the FR model (Approach II) reveals that about 7 % of the study area falls in the ‘very good’ groundwater potential zone, 31 % in the ‘good’ zone, 52 % in the ‘moderate’ zone, and 10 % in the ‘poor’ groundwater potential zone. In addition, the groundwater prospect map obtained by the WOE model (Approach II) reveals that about 3 and 41 % of the study area fall in the ‘very good’ and ‘good’ groundwater potential zones, respectively, while 48 % falls in the ‘moderate’ zone and 8 % falls in the ‘poor’ groundwater potential zone. The validation results of the two approaches suggested that the prediction accuracy of the AHP technique (Approach I) is about 77 %, that of the WOE model about 73 % and that of the FR model about 68 %.

Based on the findings of this study, it can be inferred that the performance of the AHP technique (Approach I) is

much superior to the probabilistic models (FR and WOE models), though the performance of the WOE model can be considered somewhat comparable with that of the AHP technique. Therefore, for more reliable results, the AHP technique is recommended for identifying groundwater prospect zones in a basin/sub-basin in general and in the study area in particular. If adequate data are available in an area or region for probabilistic modeling, the use of the WOE model should be preferred to the FR model. Groundwater prospect maps are very useful for the cost-effective selection of suitable sites for well drilling as well as for the effective planning and development of groundwater resources. The methodology demonstrated in this study is also applicable to other regions of the world, irrespective of hydrologic and hydrogeologic conditions.

References

- Bonham-Carter GF (1994) Geographic information systems for geoscientists: modeling with GIS. Pergamon Press, Ottawa
- Chowdhury A, Jha MK, Chowdary VM, Mal BC (2009) Integrated remote sensing and GIS-based approach for assessing groundwater potential in West Medinipur district, West Bengal, India. *Int J Remote Sens* 30(1):231–250
- Eastman JR (2003) IDRISI Kilimanjaro: guide to GIS and image processing. Clark Laboratories, Clark University, Worcester, USA
- Hinton JC (1996) GIS and remote sensing integration for environmental applications. *Int J Geogr Inf Syst* 10:877–890
- Jaiswal RK, Mukherjee S, Krishnamurthy J, Saxena R (2003) Role of remote sensing and GIS techniques for generation of groundwater prospect zones towards rural development: an approach. *Int J Remote Sens* 24(5):993–1008
- Jasrotia AS, Bhagat BD, Kumar A, Kumar R (2013) Remote sensing and GIS approach for delineation of groundwater potential and groundwater quality zones of Western Doon Valley, Uttarakhand, India. *J Indian Soc Remote Sens* 41(2):365–377
- Jha MK, Peiffer S (2006) Applications of remote sensing and GIS technologies in groundwater hydrology: past, present and future. BayCEER, Bayreuth, Germany
- Jha MK, Chowdhury A, Chowdary VM, Peiffer S (2007) Groundwater management and development by integrated remote sensing and geographic information systems: prospects and constraints. *Water Resour Manage* 21(2):427–467
- Jha MK, Chowdary VM, Chowdhury A (2010) Groundwater assessment in Salboni Block, West Bengal (India) using remote sensing, geographical information system and multi-criteria decision analysis techniques. *Hydrogeol J* 18:1713–1728
- Kim KD, Lee S, Oh HJ, Choi JK, Won JS (2006) Assessment of ground subsidence hazard near an abandoned underground coal mine using GIS. *Environ Geol* 50:1183–1191
- Krishnamurthy J, Kumar NV, Jayaraman V, Manivel M (1996) An approach to demarcate groundwater potential zones through remote sensing and a geographic information system. *Int J Remote Sens* 17(10):1867–1884
- Lee S, Choi J (2004) Landslide susceptibility mapping using GIS and the weight of evidence model. *Int J Geogr Inf Sci* 18(8):789–814
- Lee S, Dan NT (2005) Probabilistic landslide susceptibility mapping in the Lai Chau province of Vietnam: focus on the relationship between tectonic fractures and landslides. *Environ Geol* 48:778–787
- Lee S, Oh HJ, Kim KD (2010) Statistical spatial modeling of ground subsidence hazard near an abandoned underground coal mine. *Disaster Adv* 3(1):11–23
- Lee S, Kim YS, Oh HJ (2012) Application of a weights-of-evidence method and GIS to regional groundwater productivity potential mapping. *J Environ Manage* 96:91–105
- Machiwal D, Jha MK, Mal BC (2011) Assessment of groundwater potential in a semi-arid region of India using remote sensing, GIS and MCDM techniques. *Water Resour Manage* 25(5):1359–1386
- Madrucci V, Taioli F, Carlos CA (2008) Groundwater favorability map using GIS multi-criteria data analysis on crystalline terrain, Sao Paulo State, Brazil. *J Hydrol* 357:153–173
- Mays LW (2013) Groundwater resources sustainability: past, present and future. *Water Resour Manage* 27(13):4409–4424
- Meijerink AMJ (2007) Remote sensing applications to groundwater. IHP-VI, Series on groundwater No. 16, UNESCO, Paris
- Moiwo JP, Yang Y, Tao F, Lu W, Han S (2011) Water storage change in the Himalayas from the gravity recovery and climate experiment (GRACE) and an empirical climate model. *Water Resour Res* 47:W07521. doi:10.1029/2010WR010157
- Oh HJ, Lee S, Chotikasathien W, Kim CH, Kwon JH (2009) Predictive landslide susceptibility mapping using spatial information in the Pechabun area of Thailand. *Environ Geol* 57:641–651
- Oh HJ, Lee S, Soedradjat G (2010) Quantitative landslide susceptibility mapping at Pemalang area, Indonesia. *Environ Earth Sci* 60:1317–1328
- Oh HJ, Kim YS, Choi JK, Lee S (2011) GIS mapping of regional probabilistic groundwater potential in the area of Pohang City, Korea. *J Hydrol* 399:158–172
- Ozdemir A (2011) GIS-based groundwater spring potential mapping in the Sultan Mountains (Konya, Turkey) using frequency ratio, weights of evidence and logistic regression methods and their comparison. *J Hydrol* 411:290–308
- Pradhan B, Lee S (2010) Delineation of landslide hazard areas on Penang Island, Malaysia by using frequency ratio, logistic regression, and artificial neural network models. *Environ Earth Sci* 60:1037–1054
- Rodell M, Velicogna I, Famiglietti JS (2009) Satellite-based estimates of groundwater depletion in India. *Nature* 460:999–1002
- Saaty TL (1980) The analytic hierarchy process: planning, priority setting, resource allocation. McGraw-Hill, New York
- Saaty TL (2001) Decision making for leaders. RWS Publications, Pittsburgh
- Sander P, Chesley MM, Minor TB (1996) Groundwater assessment using remote sensing and GIS in a rural groundwater project in Ghana: lessons learned. *Hydrogeol J* 4(3):40–49
- Saraf AK, Choudhury PR (1998) Integrated remote sensing and GIS for groundwater exploration and identification of artificial recharge sites. *Int J Remote Sens* 19(10):1825–1841
- Scanlon BR, Longuevergne L, Long D (2012) Ground referencing GRACE satellite estimates of groundwater storage changes in the California Central Valley, USA. *Water Resour Res* 48:W04520. doi:10.1029/2011WR011312
- Sener E, Davraz A, Ozcelik M (2005) An integration of GIS and remote sensing in groundwater investigations: a case study in Burdur, Turkey. *Hydrogeol J* 13(5–6):826–834
- Solomon S, Quiel F (2006) Groundwater study using remote sensing and geographic information system (GIS) in the central highlands of Eritrea. *Hydrogeol J* 14(5):729–741
- Srivastava PK, Bhattacharya AK (2006) Groundwater assessment through an integrated approach using remote sensing, GIS and

- resistivity techniques: a case study from a hard rock terrain. *Int J Remote Sens* 27(20):4599–4620
- Tweed SO, Leblanc M, Webb JA, Lubczynski MW (2007) Remote sensing and GIS for mapping groundwater recharge and discharge areas in salinity prone catchments, southeastern Australia. *Hydrogeol J* 15(1):75–96
- Voss KA, Famiglietti JS, Lo M, Linage C, Rodell M, Swenson SC (2013) Groundwater depletion in the Middle East from GRACE with implications for transboundary water management in the Tigris-Euphrates-Western Iran region. *Water Resour Res* 49:904–914. doi:[10.1002/wrcr.20078](https://doi.org/10.1002/wrcr.20078)